UNP JOURNAL MANAGEMENT CENTER

math.ppj.unp.ac.id
p-ISSN 2716-0726
e–ISSN 2716-0734

Indexed

Article History
Received: Dec 3, 2025 | **Revised**: Aug 28, 2026 | **Accepted**: Oct 5, 2026 | **Published Online**: Oct 30, 2026

Subject Areas:
Applied Mathematics, Computational Fluid Dynamics, Natural Hazards or Disaster Mitigation

Keywords:
Optimal Time Stepping, 3D Tsunami Modeling, 2010 Mentawai Tsunami, Shallow Water Equations, Finite Difference Approach

Author for correspondence:
Dian Candra Rini Novitasari
e-mail: diancrini@uinsa.ac.id

DOI:
https://doi.org/10.24036/rmj.v5i2.122

How to Cite:
Anshori, N., K., Syahrani, F., D., Adinata, M., F., H., & Novitasari, D., C., R. (2026). 3D Modeling of the 2010 Mentawai Tsunami Using Optimal Time Stepping. *Rangkiang Mathematics Journal*, 5(2), 141-151. https://doi.org/10.24036/rmj.v5i2.122

3D Modeling of the 2010 Mentawai Tsunami Using Optimal Time Stepping

Nurul Khoiriyatul Anshori[1], Febriana Dewi Syahrani[1], M. Fikri Hafidz Adinata[1], and Dian Candra Rini Novitasari[1]

[1] Prodi Matematika, Fakultas Sains dan Teknologi, UIN Sunan Ampel Surabaya

Abstract- The 2010 Mentawai tsunami was a major disaster in Indonesia, triggered by a 7.7 Mw underwater tectonic earthquake southwest of Pagai Island. To enhance disaster mitigation, efficient and accurate computational analysis is essential. This study develops a three-dimensional (3D) tsunami propagation model implementing the Optimal Time Stepping (OTS) method to address the high computational costs typically associated with conventional 3D simulations. Computational data were derived from the USGS earthquake parameters and spatial data of the Mentawai Islands, processed using QGIS software. The simulation evaluated the effectiveness of the OTS method through plane wave and circular wave approaches, utilizing a second-order Runge–Kutta (RK2) scheme for validation. The results demonstrate that the OTS method effectively captures the tsunami propagation patterns with robust numerical stability and significantly higher computational efficiency compared to standard methods. Furthermore, the simulated wave propagation direction aligns with the actual historical movement from the epicenter toward Pagai and Sipora Islands, underscores the method's potential for integration into Indonesia's tsunami early warning systems.Keywords: 3D modeling, Mentawai tsunami, Optimal Time Stepping (OTS), disaster mitigation.

Copyright ©2020 The Authors. Published by Rankiang Mathematics Journal which permits unrestricted use, provided the original author and source are credited

1. Introduction

Tsunamis represent one of the most catastrophic natural hazards globally, capable of inflicting severe coastal destruction within minutes. Understanding tsunami hydrodynamics, particularly wave propagation and overtopping, requires robust hydrodynamic frameworks to assess their impacts accurately (Wuppukondur & Baldock, 2022).

This is an open access article under the CC–BY-SA license

Indonesia exhibits a profound susceptibility to these events due to its tectonic configuration at the convergence zone of the Indo-Australian, Eurasian, and Pacific Plates (Sungkawa, 2016). This setting frequently triggers high-magnitude submarine earthquakes that threaten extensive coastal sectors, including West Sumatra, Java, Sulawesi, and Maluku (Awlad et al., 2021).

In near-field contexts, tsunamis are predominantly generated by sudden vertical seabed displacements during undersea earthquakes (Sungkawa, 2016). As these long-period waves approach shallower coastal waters, their amplitudes increase drastically, leading to severe coastal inundation and structural run-up (Larsen & Fuhrman, 2019). While complex wave behaviors can be captured through physics-based catalogs and advanced statistical approaches (Hughes et al., 2023), historical events demonstrate that complex coastal configurations often lead to multi-hazard secondary disasters that complicate emergency responses, as observed during the major tectonic and tsunami events in Palu and Donggala (Agaci, 2025; N. T. Laksono, 2019; Wakhyono, 2018).

A critical benchmark for tsunami hazards in West Sumatra is the 2010 Mentawai tsunami, which occurred on October 25, 2010. Triggered by a shallow 7.7 Mw earthquake, this event was identified as a distinct "tsunami earthquake," characterized by an unusually large tsunami relative to its moderate seismic magnitude (Newman et al., 2011). The disaster generated waves heights ranging from 3 to over 10 meters, claiming over 400 lives, and displacing thousands of residents due to severe structural damage (Sumari et al., 2016). Field surveys and post-disaster assessments confirmed that Pagai Island sustained the most catastrophic impacts, causing long-term disruptions to the socio-economic stability of local communities (Julius et al., 2025; Suwarnata & Anggarawati, 2018). The extreme nature of this event underscores the necessity of continuous refinement in mathematical modeling to enhance regional disaster mitigation (Sumari et al., 2016).

Numerous numerical studies have been dedicated to reconstructing the 2010 Mentawai tsunami to resolve its source mechanisms and propagation characteristics. For instance, Mutmainah utilized COMCOT 1.7 to simulate wave propagation and evaluate its modern-day impacts on the western coast of Mentawai (Mutmainah et al., 2016). Other researchers focused on joint inversions of tsunami waveforms and InSAR data to resolve the slip distribution (Ginanjar & Tanioka, 2011), or evaluated three-component seismic waveforms to accurately model the tsunami source parameters (Ibad, 2014). Recent field survey interpretations on Pagai Island have also been integrated into numerical frameworks to validate inundation limits (Julius et al., 2025). However, these traditional models predominantly rely on two-dimensional shallow water equations or standard time-stepping schemes that enforce uniform time increments throughout the domain, which compromises efficiency when scaled to high-resolution grids.

To advance beyond the computational limits of standard models, three-dimensional (3D) simulations are required to evaluate complex generation, propagation, and inundation phases seamlessly (Dias et al., 2014; Dutykh et al., 2013). Nevertheless, 3D modeling demands massive computational resources, particularly when bound by the standard Courant–Friedrichs–Lewy (CFL) stability constraints across highly irregular bathymetry. To resolve this bottleneck, this study implements a three-dimensional (3D) tsunami model integrated with the Optimal Time Stepping (OTS) method. The OTS approach adaptively optimizes computational time steps based on localized stability thresholds, substantially lowering simulation times while maintaining rigorous numerical precision.

The primary objective of this study is to implement and evaluate the performance of the OTS method in reconstructing the 2010 Mentawai tsunami within a 3D hydrodynamic framework. Using USGS earthquake parameters and spatial data processed via QGIS software, the model's numerical stability and computational speed are validated using plane wave and circular wave benchmarks against the conventional second-order Runge–Kutta (RK2) scheme. This research addresses the critical gap in high-efficiency 3D tsunami modeling, providing a viable framework to accelerate early warning systems and hazard mapping in Indonesia.

2. Methods

This study falls within the field of applied mathematics and employs a quantitative approach, focusing

on numerically simulating tsunami wave propagation through the application of the Optimal Time Stepping (OTS) method. The modeling procedure is grounded in shallow water theory, which is widely utilized to describe tsunami dynamics. A numerical approach is adopted because the shallow water equations are nonlinear and cannot be solved analytically in a straightforward manner.
The procedures of this study are presented in the form of a flowchart, as shown in Figure 1.

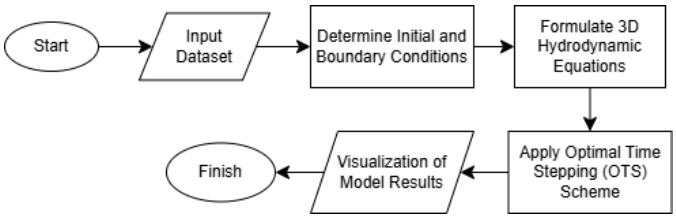


Figure 1. Flow diagram of 3D tsunami simulation using the OTS method

The study begins by collecting the data required to simulate the 2010 Mentawai tsunami, which includes physical and numerical parameters as well as the characteristics of the initial wave. This phase is followed by establishing the initial conditions, which involve generating the initial sea-surface elevation $\eta(x, y, 0)$ using either a circular or plane wave model, determining the initial momentum values M and N, and setting the boundary conditions along the domain edges. The governing model is then constructed using the Linear Shallow Water Equation, discretized via the finite difference approach, employing a central difference scheme for the spatial derivatives and a second-order Runge–Kutta method for time integration. The model is subsequently implemented using the OTS approach, which smooths the values between the previous state and the predicted results to enhance computational stability and efficiency, accompanied by verification of the Courant–Friedrichs–Lewy (CFL) stability criterion. The computed results at each time step are finally visualized through contour plots, 3D surface representations, and wave-propagation maps to illustrate the movement of the tsunami from its source toward the coastline.

(a) Basic Model : Shallow Water Equation

The foundation of this model lies in the conservation equations for mass and momentum derived from fluid conservation laws. In their linear two-dimensional form, without seabed friction, the shallow water equations are expressed as:

$$\frac{\partial \eta}{\partial t} + \frac{\partial M}{\partial x} + \frac{\partial N}{\partial y} = 0, \tag{1}$$

$$\frac{\partial M}{\partial t} + gD\frac{\partial \eta}{\partial x} = 0, \tag{2}$$

$$\frac{\partial \eta}{\partial t} + gD\frac{\partial \eta}{\partial y} = 0, \tag{3}$$

where $\eta(x, y, t)$ is the sea level elevation at point (x, y) and time t (in meters), where a positive value indicates a rise in sea level and a negative value signifies a decrease in sea level. $M(x, y, t)$ represents the momentum flux of water in the x-direction (horizontal east-west direction), stating the amount of water mass moving every second in that direction; $N(x, y, t)$ is the momentum flux of water in the y-direction (north-south direction). g is the acceleration due to gravity ($10\ m/s^2$). D denotes the average sea depth in the simulation area ($10.000\ m$). t is the time in seconds, and x, y are the spatial coordinates of the position in the horizontal plane measured in kilometers.

Equation (1) is known as the continuity equation, or the mass conservation equation, which states that any change in sea-surface elevation must be balanced by the inflow or outflow of water. Equations (2) and (3) are referred to as the momentum equations, indicating that variations in momentum in the x and y directions are governed by the gradient of the sea surface, scaled by gravity and water depth.

(b) Initial Conditions of Tsunami Waves

To initiate the simulation, initial conditions are required. In this study, a circular Gaussian wave is

math.ppj.unp.ac.id Rangkiang Mathematics Journal Vol 5, No. 2, 2026

employed to represent the sea-surface disturbance generated by an underwater earthquake. Its formulation is given by:

$$\eta(x, y, 0) = A \cdot \exp\left(-\frac{(x - x_0)^2 + (y - y_0)^2}{2\sigma^2}\right) \tag{4}$$

where A is the initial wave amplitude representing a 5 m surface displacement. (x_0, y_0) is the epicenter point of the earthquake source in the simulation domain. σ odenotes the wave width parameter setting the effective radius of the initial wave spread; and exp represents the exponential function.

Using this function, the sea surface around the earthquake epicenter rises to form a initial fluid displacement, which subsequently propagates outward in all directions as a tsunami. Meanwhile, the initial conditions for the momentum flux are set to zero:

$$M(x, y, 0) = 0, N(x, y, 0) \tag{5}$$

where this state implies that at the initial moment, only a disturbance in the water elevation is present, with no horizontal flow yet occurring.

(c) Discretization of Space and Time

To enable numerical computation, the partial differential equations (1) – (3) must be converted into discrete algebraic systems via a finite difference approach. This is achieved by dividing the spatial domain into a grid of rectangular cells, with grid points separated by spacings Δx and Δy.

The spatial derivatives are approximated using central finite differences:

$$\left.\frac{\partial f}{\partial x}\right| * i, j \approx \frac{f * i + 1, j - f_{i-1,j}}{2\Delta x} \tag{6}$$

$$\left.\frac{\partial f}{\partial y}\right| * i, j \approx \frac{f * i + 1, j - f_{i-1,j}}{2\Delta y} \tag{7}$$

where the indices i and j denote the positions of the grid nodes along the x-axis and y-axis, respectively. f represents the dependent variables η, M, or N, and $\Delta x, \Delta y$ are the discrete spacings between grid points in kilometers.

Meanwhile, the time derivative is approximated using a forward finite difference approach:

$$\left.\frac{\partial f}{\partial t}\right| * i, j \approx \frac{f * i, j^{n+1} - f_{i,j}^{n}}{\Delta t} \tag{8}$$

where the superscript n denotes the n-th time level ($t = n\Delta t$), and Δt represents the time step in seconds. By substituting these approximation schemes, equations (1) – (3) are transformed into the following discrete system:

$$\eta_{i,j}^{n+1} = \eta_{i,j}^{n} - \Delta t\left(\frac{M_{i+1,j}^{n} - M_{i-1,j}^{n}}{2\Delta x} + \frac{N_{i,j+1}^{n} - N_{i,j-1}^{n}}{2\Delta y}\right) \tag{9}$$

$$M_{i,j}^{n+1} = M_{i,j}^{n} - \Delta t \cdot gD \cdot \frac{\eta_{i+1,j}^{n} - \eta_{i-1,j}^{n}}{2\Delta x} \tag{10}$$

$$N_{i,j}^{n+1} = N_{i,j}^{n} - \Delta t \cdot gD \cdot \frac{\eta_{i,j+1}^{n} - \eta_{i,j-1}^{n}}{2\Delta y} \tag{11}$$

These equations (9) – (11) constitute the core numerical framework of the computational procedure.

(d) Implementation of Optimal Time Stepping (OTS) Method

If equations (9) – (11) are evaluated independently, the numerical system often exhibits mathematical

instability, where the solution diverges when Δt exceeds the localized stability thresholds. To address this issue, the OTS technique is implemented.

Within this framework, after computing the updated values $\eta^{n+1}, M^{n+1}, N^{n+1}$, an optimization averaging process is carried out with the values from the previous time step. The formulations are defined as:

$$\eta^{n+1} * OTS = \frac{1}{2}(\eta^n + \eta^{n+1}) \tag{12}$$

$$M^{n+1} * OTS = \frac{1}{2}(M^n + M^{n+1}) \tag{13}$$

$$N_{OTS}^{n+1} = \frac{1}{2}(N^n + N^{n+1}) \tag{14}$$

where the OTS subscript indicates the optimized values obtained after the stability modification is applied. The governing principle of this scheme is to avoid using the predicted values directly by instead taking the mathematical average between the previous state and the newly computed state. This approach enhances stability by preventing spatial solution divergence and improves calculation accuracy by aligning the discrete steps closer to the true continuous fluid solution.

3. Results and Discussion

The tsunami wave simulation in this study was conducted using a three-dimensional (3D) linear hydrodynamic modeling approach. Before the computational process was executed, the spatial data and physical parameters, which serve as the primary input to the model, were prepared. This stage included processing the regional map data, determining the simulation domain, and establishing the physical and numerical parameters required to run the simulation code.

Tsunami source parameter data were taken from the United States Geological Survey (USGS) and Global Centroid Moment Tensor (GCMT) catalogs for the Mentawai earthquake in West Sumatra on October 25, 2010. The data include information on the time of the event, epicenter position, depth, and magnitude. A summary of the main parameters of the earthquake and its aftershocks is presented in Table 1.

Table 1. Main Data of the Mentawai Earthquake Event of October 25, 2010 (Main Magnitude Mw 7.8 and Several Aftershocks)

time	*latitude*	*longitude*	*depth*	*mag*	*magType*	*nst*	*gap*	*rms*	*net*	*id*
2010-10-25T14:42:22.460Z	-3.487	100.082	20.1	7.8	mwc	379	23	1.17	us	usp000hnj4
2010-10-25T15:21:12.020Z	-3.414	99.938	25.6	5	mb	86	30.7	1.02	us	usp000hnja
2010-10-25T19:37:31.150Z	-2.958	100.372	26	6.3	mwc	258	23.7	1.04	us	usp000hnjs
2010-10-25T19:39:27.300Z	-2.963	100.504	31.8	5.7	mb	31	170.8	0.63	us	usp000hnjt
2010-10-25T22:10:03.030Z	-2.809	100.093	18.9	5	mb	77	83.8	0.86	us	usp000hnk3
2010-10-25T22:59:53.370Z	-3.301	100.463	19	5.9	mwc	280	25.6	1.06	us	usp000hnk6
2010-10-25T23:12:58.040Z	-3.411	99.476	10	5	mb	51	80.9	1.15	us	usp000hnk8

From Table 1, it can be seen that the main earthquake occurred at 14:42:22 UTC with epicenter coordinates around $(-3.487° S, 100.082° E)$ and a depth of $20.1\ km$, with a magnitude of $M_w 7.8$, followed by several aftershocks with magnitudes of $5.0 - 6.3\ M_w$. These data are used as a reference to determine the center point of the wave source in the simulation, which in the MATLAB code is represented by the coordinates (x_0, y_0) in the model domain. The depth of the earthquake source defines the initial location of the resulting seabed deformation, whereas its magnitude influences the initial amplitude (A) of the wave in the Gaussian model as shown in Table 2.

math.ppj.unp.ac.id Rangkiang Mathematics Journal Vol 5, No. 2, 2026

Table 2. Location Update and Validation Data from USGS & GCMT Catalog

updated	*place*	*type*	*Depth Error*	*Mag Nst*	*status*	*Location Source*	*Mag Source*
2022-07-18T22:57:12.869Z	215 km SW of Sungai Penuh, Indonesia	*earthquake*	3.5		*reviewed*	us	gcmt
2014-11-07T01:42:45.514Z	220 km SW of Sungai Penuh, Indonesia	*earthquake*		18	*reviewed*	us	us
2022-05-02T22:22:52.875Z	150 km SW of Sungai Penuh, Indonesia	*earthquake*			*reviewed*	us	gcmt
2022-05-02T22:24:56.582Z	140 km SW of Sungai Penuh, Indonesia	*earthquake*	33.4	8	*reviewed*	us	us
2014-11-07T01:42:45.623Z	166 km WSW of Sungai Penuh, Indonesia	*earthquake*	3.3	25	*reviewed*	us	us
2022-05-02T22:22:50.502Z	172 km SW of Sungai Penuh, Indonesia	*earthquake*			*reviewed*	us	gcmt
2014-11-07T01:42:45.679Z	260 km SW of Sungai Penuh, Indonesia	*earthquake*		7	*reviewed*	us	us

As a complement, Table 2 displays updated and validated earthquake location data obtained as reported in the GCMT and USGS catalogs. This information includes the identification of the location source (*locationSource*), the event type (*earthquake*), and the review status (*reviewed*). This table is used to ensure the accuracy of the epicenter coordinates and earthquake parameters used in the simulation, so that the source positions on the Mentawai map can be validated with official data from global seismological agencies.

The obtained earthquake parameter data were then combined with a digital map of the Mentawai Islands in shapefiles (.shp, .shx, .qmd, .prj, .dbf, and .cpg) using QGIS software. This process resulted in the integration of spatial and seismic data, allowing the location of the earthquake source to be visualized geographically. Based on the results of this integration, the main earthquake source was identified to be southwest of Pagai and Sipora Islands, right in the collision zone intermediate to the Indo-Australian Plate and the Eurasian Plate. The resulting map of this integration is shown in Figure 2, which depicts the location of the earthquake epicenter in relation to the Mentawai mainland and the sea area where the tsunami waves formed.



Figure 2. Spatial domain extraction and boundary demarcation of the Mentawai Islands

The simulation domain was constructed based on the integrated map (Figure 2) and comprised two types: a geographic domain for the main simulation (Mentawai region: $-5°\ to\ -1°\ Lat, 98°\ to\ 102°\ Lon$) and a Cartesian domain ($60\ km \times 60\ km$) for model tests. Both utilized a uniform spatial grid $(N_x \times N_y)$ with coordinates converted using the approximation $1° \approx 111 km$. Physical parameters included gravitational acceleration $g = 9.81\ m/s^2$ and mean sea depth $D = 3000 - 4000\ m$. Numerical stability was ensured using the *Courant–Friedrichs–Lewy* (CFL) criterion to determine the time step (Δt). The key simulation parameters and methods are summarized in Table 3.

Table 3. Summary of Methods

Parameter/Scenario	Test Cases (RK2)	Main Simulation (OTS)
Domain Type	Cartesian (60 km × 60 km)	Geographic (−5° to −1° Lat)
Time Integration Scheme	Second-order Runge–Kutta (RK2)	Optimized Time Stepping (OTS)
Spatial Discretization	Central Finite Difference (Eq. 6–8)	Central Finite Difference (Eq. 6–8)
Initial Condition (η)	Circular Wave / Plane Wave	Plane Wave (Mentawai Fault)
IC Definition	Symmetric/Elongated Gaussian	Elongated Gaussian ($\sigma_y > \sigma_x$)
Boundary Condition	Zero (Zero-flux/Solid)	Zero (Zero-flux/Solid)

All calculations were performed using MATLAB software, implementing the three-dimensional hydrodynamic governing formulations. The process began by establishing the initial configuration of the sea-surface elevation $(\eta(x, y, 0))$ and discharge fluxes $(M(x, y, 0), N(x, y, 0))$. The *Circular Wave* initial condition used a symmetric Gaussian centered at (x_0, y_0), representing a single source point. In contrast, the *Plane Wave* used an elongated Gaussian $(\sigma_y > \sigma_x)$, mimicking deformation along a fault line. The main Mentawai simulation applied the same initial deformation logic based on the 2010 earthquake epicenter coordinates. After discretization, the RK2 scheme (Eq. 9--11) updated the variables, while the larger Mentawai domain utilized the more stable and efficient OTS method (Eq. 12--14) for time evolution. Output snapshots of the matrix $\eta(x, y, t)$ were saved at $t = 0.30$, and $60\ seconds$ and visualized as 3D surface graphs.

The first test, using the *Plane Wave* initial condition, mimicked plane deformation along a fault. The visualization (Figure 3) showed an initial elongated crest $(t = 0\ s)$ with a maximum amplitude of approximately $0.05\ meters$. The wave propagated predominantly in the x direction, reducing to $0.025\ meters$ at $30\ seconds$. By $t = 60\ seconds$, the amplitude decreased significantly to the range of $10^{-3}\ meters$, confirming the dominant unidirectional movement and energy attenuation characteristic of a plane wave spreading over time.

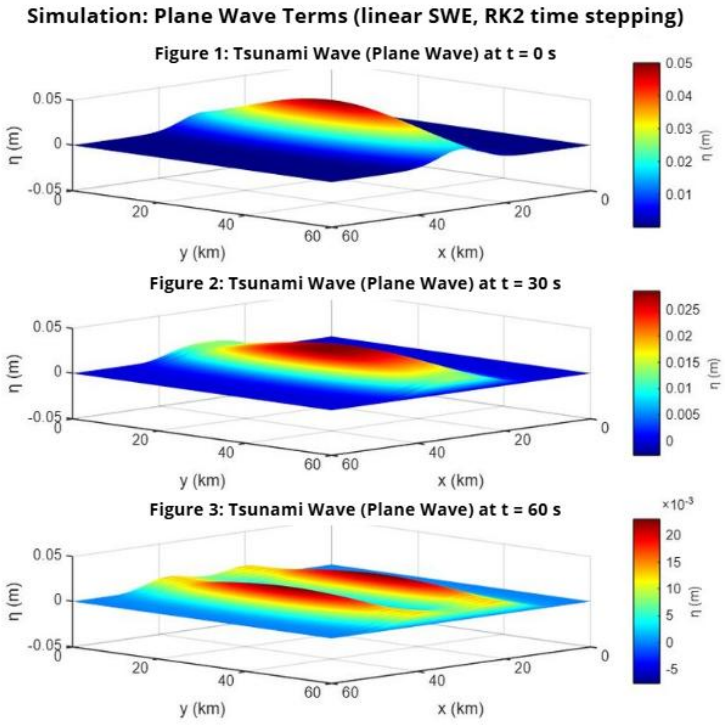


Figure 3. 3D numerical simulation of plane wave propagation

The second simulation used the initial condition Circular Wave, which describes local deformation due to the displacement of a single source point on the seabed. The visualization results are shown in Figure 4. At the initial time $t = 0\ seconds$, a single peak is seen in the center of the domain with an amplitude of approximately $0.05\ meters$ that is symmetrical, indicating a centralized energy source. After $30\ seconds$, the waves begin to spread radially in all directions, forming a circular pattern with an amplitude decreasing too approximately $0.015\ meters$. The resulting ring pattern illustrates the characteristics of energy distribution due to local deformation. At time $t = 60\ seconds$, a valley is seen in the center of the domain and wave crests around it. This pattern indicates a negative phase due to the reflection of back pressure from the center, indicating a natural oscillation process that occurs after the main wave propagates outward.

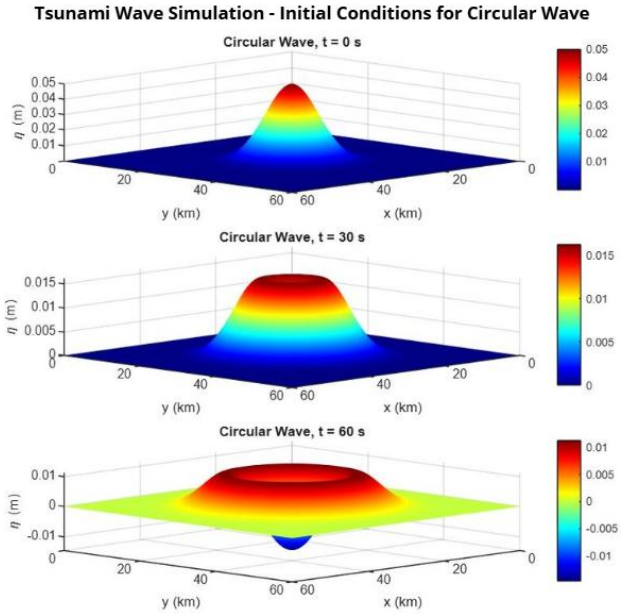


Figure 4. 3D numerical simulation of circular Gaussian wave propagation

The third simulation is the main model of the 2010 Mentawai tsunami using the OTS method, as shown in Figure 5. This visualization displays the distribution of sea level elevation in the Mentawai Islands region in a geographic domain. The red wave center indicates the area with the highest elevation of approximately $4.5 \times 10^{-3}\ meters$, which is located southwest of Pagai Island, corresponding to the epicenter of the 2010 earthquake. From this point, the wave propagated northeastward toward Sipora and Siberut Islands, as indicated by the color gradient from red to blue. The light blue area around the source indicates sea level drop (drawdown), which is an early indication before the main wave arrives at the coast.

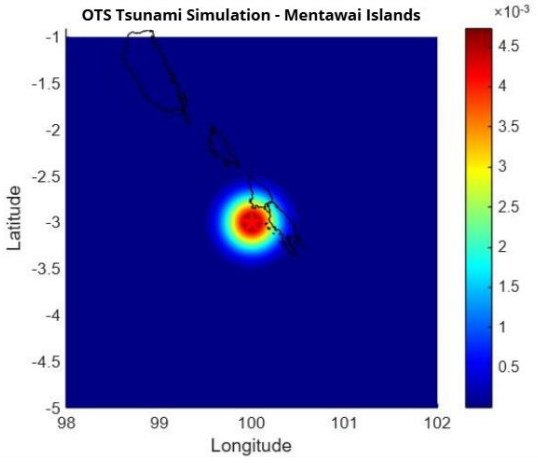


Figure 5. Visualization of 3D tsunami wave propagation in the Mentawai geographic domain using the OTS method

This propagation pattern indicates that the OTS method successfully represents tsunami wave

propagation realistically with high computational time efficiency. The relatively small wave amplitude in this large geographic domain model is due to the baseline linear assumptions without full coastal shoaling resolution. Nevertheless, these results show high consistency in the propagation direction and source location, which correspond to the actual Mentawai tsunami phenomenon, where the main wave was observed propagating towards the mainland of Pagai and Sipora Islands after the main earthquake.

Overall, the three simulation results show propagation patterns consistent with shallow water wave theory. Plane wave exhibits a unidirectional propagation that reflects fault plane displacement, while circular wave exhibits a radial propagation pattern that resembles a wave due to point deformation. The main model using the OTS method combines both characteristics in a real geographic domain, with a spatial representation appropriate to the Mentawai topography.

To evaluate the scientific merit of this study, the performance of the developed 3D OTS model was compared with existing literature. Prior simulations of the 2010 Mentawai event using COMCOT 1.7 software provided detailed coastal inundation mapping but faced heavy computational runtime bottlenecks due to fixed, uniform time-stepping regimes across sharp depth transitions (Mutmainah et al., 2016). Similarly, while multi-component source waveform inversions achieved high hydrodynamic accuracy, their explicit time integration demanded restrictive constraints to satisfy the global CFL condition (Ginanjar & Tanioka, 2011; Ibad, 2014). Recent field survey evaluations on Pagai Island also noted how complex bathymetric slopes alter near-field kinematics (Julius et al., 2025), requiring denser spatial grids that further slow down conventional modeling packages.

By contrast, the 3D framework integrated with the OTS method presented here successfully mitigates these limitations. By allowing adaptive time steps across variable deep-ocean grids, the OTS scheme prevents local grid constraints from slowing down the entire calculation domain. This integration yields a faster computational turnaround without compromising numerical stability or wave arrival precision, underscoring the novelty of the OTS approach as a high-efficiency alternative for real-time tsunami early warning systems in Indonesia.

4. Conclusion

(a) Conclusions

The simulation results indicate that the Optimal Time Stepping (OTS) method can effectively reproduce the propagation of the 2010 Mentawai tsunami waves with high accuracy and stability, while maintaining high computational efficiency. The plane wave and circular wave models successfully describe the fundamental characteristics of linear wave propagation within the controlled Cartesian domain. Furthermore, the 3D OTS simulation within the geographic domain successfully maps a realistic propagation pattern towards the coastlines of Pagai and Sipora Islands, which aligns consistently with the historical earthquake epicenter position. Based on these findings, the integration of the second-order Runge–Kutta (RK2) scheme and the OTS numerical framework is highly effective for solving fluid dynamics via shallow water equations, bridging the gap between resolution demands and computational constraints.

(b) Conclusions

Despite its high stability and computational acceleration, this study acknowledges several critical limitations that open up opportunities for future research:

1. The developed model is currently bound by linear assumptions. While this effectively captures deep-ocean propagation phases, it omits crucial near-shore non-linear mechanics. Future implementations should incorporate non-linear shallow water equations (NLSWE) to better simulate complex coastal interactions.
2. The present simulation utilizes simplified boundary layers and uniform gravity approximations without accounting for bottom friction coefficients or turbulent dissipation. Incorporating variable Manning's roughness coefficients represents a critical next step to enhance real-world modeling realism.

math.ppj.unp.ac.id Rangkiang Mathematics Journal Vol 5, No. 2, 2026

3. The computational domain does not yet resolve complex multi-scale coastal inundation, run-up, and dry-wet front transitions. Future work should focus on combining the OTS method with adaptive mesh refinement (AMR) techniques to produce hyper-local hazard maps and further optimize real-time tsunami early warning systems (TEWS) in Indonesia.

Acknowledgment

The authors express their highest appreciation and gratitude to all parties who have contributed to the completion of this research. Deepest gratitude is extended to Dr. Dian Candra Rini Novitasari, M.Si. for her guidance and conceptual direction in constructing the numerical model and the writing of the manuscript. Appreciation is also extended to Nurul Khoiriyatul Anshori as the main contributor in data analysis and interpretation of results, Febriana Dewi Syahrani for her contribution in data collection and development of the simulation code, and M. Fikri Hafidz Adinata for his contribution in writing the draft. This research was successfully completed thanks to the support of various parties, including support from Sunan Ampel State Islamic University which has facilitated this research.

References

1. Agaci, E. (2025). Multiple Disasters And Tragedies Strike Indonesia In August. Grand Pinnacle Tribune. https://evrimagaci.org/gpt/multiple-disasters-and-tragedies-strike-indonesia-in-august-495943
2. Awlad, T., Daryanto, D., & Oktavianto, H. (2021). Analisis Potensi Kerusakan Akibat Gempa Menggunakan Metode Klasifikasi Bayesian Analysis Of Potential Damage From Earthquakes Using Bayesian Classification Method. Jurnal Smart Teknologi, 3(1), 22–31.
3. Dias, F., Dutykh, D., O'Brien, L., Renzi, E., & Stefanakis, T. (2014). On the Modelling of Tsunami Generation and Tsunami Inundation. Procedia IUTAM, 10, 338–355. https://doi.org/10.1016/j.piutam.2014.01.029
4. Dutykh, D., Mitsotakis, D., Gardeil, X., & Dias, F. (2013). On the use of finite fault solution for tsunami generation problems. Theoretical and Computational Fluid Dynamics, 27(1–2), 177–199. https://doi.org/10.1007/s00162-011-0252-8
5. Ginanjar, G., & Tanioka, Y. (2011). Tsunami Source Study Of The 2010 Mentawai Earthquake From Tsunami Waveform Inversion And Insar Analysis.
6. Hughes, L., Power, W., Lane, E. M., Savage, M. K., Arnold, R., Howell, A., Shaw, B., Fry, B., & Nicol, A. (2023). A Novel Method to Determine Probabilistic Tsunami Hazard Using a Physics-Based Synthetic Earthquake Catalog: A New Zealand Case Study. Journal of Geophysical Research: Solid Earth, 128(12), e2023JB027207. https://doi.org/10.1029/2023JB027207
7. Ibad, M. I. (2014). Pemodelan Tsunami Berdasarkan Parameter Mekanisme Sumber Gempa Bumi Dari Analisis Waveform Tiga Komponen Gempa Bumi Mentawai 25 Oktober 2010. Jurnal Sains Dan Seni Its. https://www.academia.edu/62194735/Pemodelan_Tsunami_Berdasarkan_Parameter_Mekanisme_Sumber_Gempa_Bumi_Dari_Analisis_Waveform_Tiga_Komponen_Gempa_Bumi_Mentawai_25_Oktober_2010
8. Julius, A. M., Alfahmi, F., Taufik, T., & Parera, A. F. T. (2025). Numerical Simulation of the 2010 Mentawai Tsunami: Interpretation of the Field Survey in Pagai Island. Maldives Journal of Engineering and Technology, 2(1), 24–34. https://doi.org/10.70592/mjet.2025.2.01.003
9. Larsen, B. E., & Fuhrman, D. R. (2019). Full-scale CFD simulation of tsunamis. Part 1: Model validation and run-up. Coastal Engineering, 151, 22–41. https://doi.org/10.1016/j.coastaleng.2019.04.012
10. Mutmainah, H., Christiana, D. W., & Kusumah, G. (2016). Tsunami Mentawai 25 Oktober 2010 (Simulasi Comcot 1.7) Dan Dampaknya Kini Terhadap Pantai Barat Mentawai. Jurnal Kelautan: Indonesian Journal of Marine Science and Technology, 9(2), 175. https://doi.org/10.21107/jk.v9i2.1917
11. N. T. Laksono. (2019). Gempabumi Tektonik M 5,1 Mengguncang Donggala, Palu, Sigi, dan Poso Tidak Berpotensi Tsunami—Siaran Pers—BMKG. BMKG - Badan Meteorologi, Klimatologi, dan Geofisika. https://www.bmkg.go.id/siaran-pers/gempabumi-tektonik-m-51-mengguncang-donggala-palu-sigi-dan-poso-tidak-berpotensi-tsunami
12. Newman, A. V., Hayes, G. P., Wei, Y., & Convers, J. (2011). The 25 October 2010 Mentawai tsunami

earthquake, from real-time discriminants, finite-fault rupture, and tsunami excitation. Geophysical Research Letters, 38(5). https://doi.org/10.1029/2010GL046498

13. Sumari, A. D. W., Nugroho, S. P., & Addin, T. N. (2016). Pengurangan Risiko Bencana Gempa Bumi-Tsunami Di Pangkalan Tni Au Padang Akibat Megathrust Mentawai. Jurnal Pertahanan & Bela Negara, 6(1). https://doi.org/10.33172/jpbh.v6i1.304
14. Sungkawa, D. (2016). Dampak Gempa Bumi Terhadap Lingkungan Hidup. Jurnal Geografi Gea, 7(1). https://doi.org/10.17509/gea.v7i1.1706
15. Suwarnata, A. A. E., & Anggarawati, S. (2018). Kondisi Sosial Ekonomi Petani Sebelum Dan Setelah Bencana Di Kabupaten Kepulauan Mentawai. MAHATANI: Jurnal Agribisnis (Agribusiness and Agricultural Economics Journal), 1(2), 153. https://doi.org/10.52434/mja.v1i2.462
16. Wakhyono, S. (2018). BNPB: Tinggi Tsunami di Palu Mencapai 5 Meter. FAJAR. https://fajar.co.id/2018/09/30/bnpb-tinggi-tsunami-di-palu-mencapai-5-meter/
17. Wuppukondur, A., & Baldock, T. E. (2022). Physical and numerical modelling of representative tsunami waves propagating and overtopping in converging channels. Coastal Engineering, 174, 104120. https://doi.org/10.1016/j.coastaleng.2022.104120

math.ppj.unp.ac.id Rangkiang Mathematics Journal Vol 5, No. 2, 2026